

Production of Highly Homogeneous Si(100) Surfaces by H₂O Etching: Surface Morphology and the Role of Strain

Marc F. Faggin,[†] Sara K. Green,[‡] Ian T. Clark,[†] K. T. Queeney,[§] and
Melissa A. Hines^{*†}

*Department of Chemistry, Cornell University, Ithaca, New York 14853-1301, and
Picker Engineering Program and Department of Chemistry, Smith College,
Northampton, Massachusetts 01063*

Received March 30, 2006; E-mail: Melissa.Hines@cornell.edu

Abstract: The etching of Si(100) surfaces in ultrapure water was studied with a combination of infrared spectroscopy (FTIR) and scanning tunneling microscopy (STM). While the FTIR results show that the initially rough H/Si(100) surface becomes highly homogeneous during etching, a phenomenon generally associated with surface smoothing, STM images reveal that the homogeneity is associated with the formation of well-defined etch hillocks. After many hours of etching, the resulting H-terminated surface is composed of stripes of atomically flat Si(100) terminated by etch hillocks bounded by {111}- and {110}-oriented microfacets. Polarization analysis of the Si–H stretching modes provides strong evidence for uniform dihydride-termination of the flat regions, with the narrow (~25 Å) width of these stripes allowing for relaxation of steric strain between neighboring dihydrides. The unusual hill-and-valley etch morphology is attributed to the effects of steric strain on the reactivity of sites on the etched surface.

1. Introduction

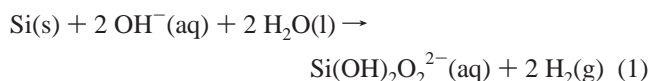
The production of ultraclean, atomically flat (or nearly atomically flat) Si(100) wafers is an important and long-standing technological challenge, as Si(100) wafers are the basis for almost all of today's microelectronic devices. Engineers have long known that even atomic-scale roughness in the Si(100)/SiO₂ interface that defines the channel/insulator junction of field-effect transistors (FETs) can adversely affect device performance. Although this roughness can be introduced in many different stages of fabrication, even the most mundane step of processing—the initial cleaning of the wafer in an aqueous solution—can play a crucial role. For example, Ohmi et al.¹ showed that the small increase in wafer roughness (from 2 to 10 Å rms) induced by aggressive, industry-standard cleaning solutions decreased channel mobility in transistors fabricated from these wafers by a factor of 4. This observation and others like it have prompted an intense search for an etchant that produces atomically flat Si(100) surfaces.²

From a chemical standpoint, the production of atomically flat surfaces appears straightforward. One would seem to need a highly *anisotropic etchant* that removes defect sites, such as steps and kinks, much more rapidly than terrace sites. Following this reasoning, an etchant that produces an atomically flat (close-packed) surface, such as Si(100), would be expected to etch

surfaces vicinal to this plane, which have an intrinsically high density of defect (step) sites, much faster than the flat surface. This simple paradigm works well for Si(111)—an economically unimportant face of silicon. As originally shown by Higashi et al.,³ Si(111) surfaces can be etched to near-atomic perfection by an aqueous solution of NH₄F. As expected, this etchant attacks defect sites more than 10⁴ times faster than terrace sites.⁴ Ultra-smooth Si(111) surfaces can also be produced with other aqueous bases, such as KOH and tetramethylammonium hydroxide (TMAH); their reactivity follows the same expected trend.

If the process is so simple, why has the production of atomically flat Si(100) surfaces stymied researchers? For example, both KOH and TMAH display pronounced etch rate minima at the (100) and (111) orientations,⁵ and vicinal Si-(100) and (111) surfaces display markedly higher etch rates than their corresponding flat surfaces. Both etchants therefore seem to satisfy the postulated criteria for the production of atomically flat (100) and (111) surfaces. Why, then, do these etchants produce near-perfect Si(111) surfaces but rough Si(100) surfaces?

Because of its tremendous economic importance, the chemistry of anisotropic etching has been intensively studied.⁶ Although the mechanism of silicon etching in strong bases remains controversial, the net reaction is believed to be



This simple formula belies the complexity of silicon etching, as it does not explain the dramatic changes in etch rate, etch

[†] Cornell University.

[‡] Picker Engineering Program, Smith College.

[§] Department of Chemistry, Smith College.

(1) Ohmi, T.; Kotani, K.; Teramoto, A.; Miyashita, M. *IEEE Electron Dev. Lett.* **1991**, *12*, 652.

(2) Higashi, G. S.; Chabal, Y. J. In *Handbook of Semiconductor Wafer Cleaning Technology*; Kern, W., Ed.; Noyes Publications: East Windsor, NJ, 1993; pp 433–496.

morphology, and etch anisotropy observed with even small changes in concentration, temperature, or cation.⁵

In this study, we approach the chemistry of anisotropic Si(100) etching with a simplifying tactic. Instead of studying the steady-state reaction under industrial conditions (i.e., high concentration, temperature, pH, and etch rate), we study the very earliest stages of etching under the simplest possible conditions. We avoid the cation problem by studying etching in pure H₂O, the only reactant necessary for reaction 1. In pure H₂O, silicon etching is presumably driven by 10⁻⁷ M of autodissociated OH⁻. The very low etch rate of this system also enables accurate time-dependent chemical studies.

In the following, we use a combination of vibrational spectroscopy and scanning tunneling microscopy to show that the simplest possible aqueous etchant—pure H₂O—can produce Si(100) surfaces of surprising and unprecedented homogeneity, such as the one shown in Figure 1. Although not perfectly flat, the etched surface is characterized by rectangular regions of atomic perfection. More importantly, this study also uncovers a flaw in the simple paradigm for the production of flat surfaces described above—a flaw that has important implications for the development of an industrially viable Si(100) etchant. In the case of Si(100), we show that the strain inherent in large regions of atomically flat Si(100) leads to kinetic roughening of the surface during etching. This roughening manifests itself in the production of nanoscale hillocks terminated by both exceedingly fast etching Si{110} and exceedingly slow etching Si{111} microfacets. The competition between defect removal and hillock formation leads to highly time-dependent etch morphologies, with the smoothest surfaces being produced at intermediate etch times.

2. Experimental Section

The exceptionally low etch rate of the H₂O/Si system introduces experimental challenges. For example, dissolved O₂ slowly oxidizes etched silicon surfaces.^{7,8} In typical etching reactions, this reaction is too slow to have significant effect. In pure H₂O, though, this reaction causes severe complications that we have avoided by working in a O₂-free environment. For similar reasons, this reaction is sensitive to extremely low levels of contamination (e.g., metal cations), which necessitates careful attention to the quality of the reagents as well as all cleaning procedures.

Substrates for infrared analysis were prepared from double-side polished, *p*-type, >1500 Ω-cm, 500-μm-thick, float-zone Si(100) wafers (Montco Silicon), whereas STM substrates were prepared from single-side polished, *p*-type, 1–20 Ω-cm Czochralski Si(100) wafers (Virginia Semiconductor). Prior to use, wafers were oxidized in O₂ (g) at 1100 °C for 45 min and then annealed under N₂ at 1100 °C for 30 min to produce a well annealed, ~1000-Å-thick SiO₂ layer. The wafers were diced into 0.6'' × 1.5'' rectangles for spectroscopic study and 0.6'' × 0.7'' samples for STM investigations. The short ends of the infrared samples were polished to form 45° entrance bevels.

Before each experiment, the silicon sample and all labware were scrupulously cleaned using a modified RCA clean.² The labware, which was either glass or solid Teflon, was cleaned in a basic peroxide solution

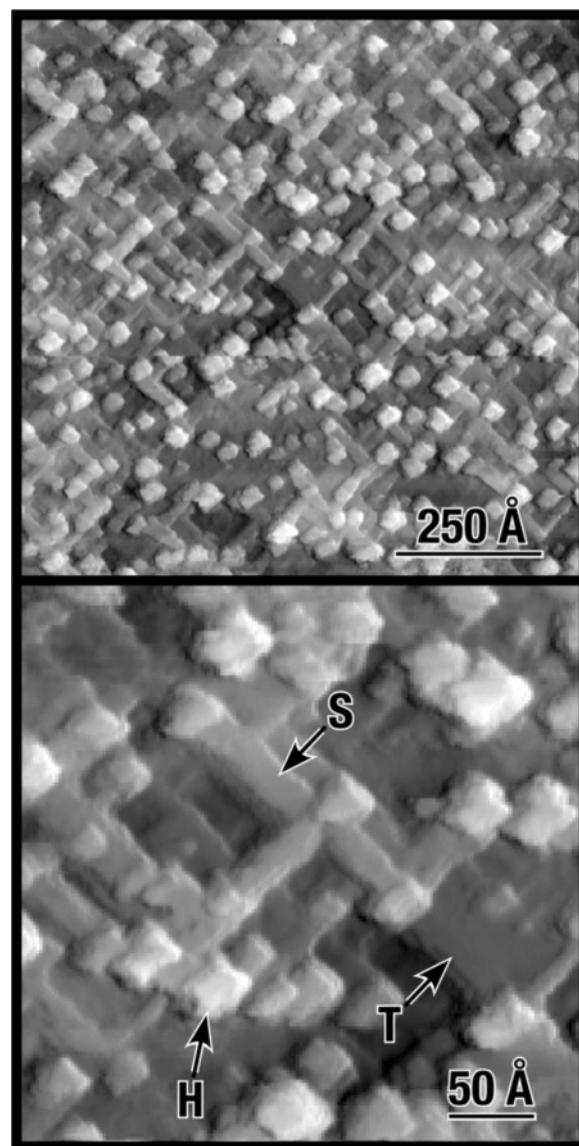


Figure 1. Two STM images of a Si(100) surface etched for 11 h in room-temperature deoxygenated H₂O. The surface displays a number of characteristic features, including raised stripes (S), hillock (H), and atomically flat terraces (T).

(SC-1) composed of 1:1:4 by volume of 28% NH₃(aq): 30% H₂O₂(aq): H₂O at 80 °C for at least 10 min and then rinsed thoroughly in running ultrapure water (Millipore Milli-Q). The sample was then cleaned in a fresh SC-1 bath for 10 min and rinsed, followed by cleaning in an acidic peroxide solution (SC-2) composed of 1:1:4 by volume of 37% HCl(aq): 30% H₂O₂(aq): H₂O at 80 °C for 10 min. The oxide layer was removed by a 2 min immersion in 5:1 buffered oxide etch (BOE, J.T Baker) and rinsed to produce a very clean, H-terminated surface for etching studies.

Cleaned samples were rapidly introduced into a closed glass container filled with deionized water and purged with argon (Airgas, ultrahigh purity). A custom Teflon sample holder permitted multiple samples to be cleaned and etched at the same time, which was crucial both for time-progression studies as well as simultaneous STM/FTIR studies. After etching, an InGa ohmic contact was applied to the backside of all STM samples. The samples were then load-locked into a ultrahigh vacuum (UHV) STM or a Ar-purged infrared spectrometer.

Spectra were acquired in the multiple internal reflection (MIR) geometry using a Nicolet 670 FTIR spectrometer equipped with a mercury–cadmium–telluride (MCT) detector and a ZnSe grid polarizer

(3) Higashi, G. S.; Chabal, Y. J.; Trucks, G. W.; Raghavachari, K. *Appl. Phys. Lett.* **1990**, *56*, 656.

(4) Hines, M. A. *Annu. Rev. Phys. Chem.* **2003**, *54*, 29.

(5) Wind, R. A.; Jones, H.; Little, M. J.; Hines, M. A. *J. Phys. Chem. B* **2002**, *106*, 1557.

(6) For a comprehensive review, see Sangwal, K. *Etching of Crystals: Theory, Experiment and Application*; North-Holland: Amsterdam, 1987.

(7) Wade, C. P.; Chidsey, C. E. D. *Appl. Phys. Lett.* **1997**, *71*, 1679.

(8) Garcia, S. P.; Bao, H.; Manimaran, M.; Hines, M. A. *J. Phys. Chem. B* **2002**, *106*, 8258.

(Molelectron) at 0.5 cm^{-1} resolution. The incident IR beam was focused onto the entrance bevel of the sample, where it underwent ~ 75 internal reflections before exiting the opposite bevel. After each spectroscopic study, the samples were oxidized in situ with a 10-min exposure to $\text{O}_3(\text{g})$ generated by a Hg discharge lamp,⁹ and a reference spectrum was obtained. Interference fringes in the spectra were removed computationally.¹⁰ Since the region below 1500 cm^{-1} is obscured in the MIR geometry by strong multiphonon bulk absorptions, transmission spectra were also taken with 2.0 cm^{-1} resolution to obtain information on the important bend and scissor modes.

3. Results

Consistent with previous investigations of $\text{H}_2\text{O}/\text{Si}(100)$ ^{11–13} and $\text{H}_2\text{O}/\text{Si}(111)$ ¹⁴ etching, the vibrational spectra of H_2O -etched surfaces show that etching produces an entirely H-terminated surface. Infrared spectra of H_2O -etched surfaces invariably show pronounced absorption bands in three characteristic regions: $615\text{--}660\text{ cm}^{-1}$ (Si–H bend vibrations), $900\text{--}920\text{ cm}^{-1}$ (SiH₂ scissor vibrations), and $2050\text{--}2150\text{ cm}^{-1}$ (Si–H stretch vibrations). No oxidation occurs during etching, as evidenced by the absence of the characteristic vibrational features due to $\text{O}_3\text{Si-H}$, SiO_2 , or SiOH species.

In contrast to previous observations,^{11–13} our experiments yielded relatively narrow line widths, particularly for H/Si(100) stretch vibration, allowing us to resolve contributions from individual surface species (vide infra). Nevertheless, the complexity of the etched surface leads to corresponding spectral complexity. For this reason, the raw spectra obtained with polarized or unpolarized radiation are complicated and difficult to assign unambiguously. The spectra can be significantly simplified using a simple computational technique, described in Section 3.1, that isolates vibrational modes oriented parallel and perpendicular to the etched surface. The assignment of these spectra and their temporal evolution is discussed in Section 3.2. Finally, STM images of the etched surfaces are presented in Section 3.3.

3.1. Polarization Analysis of Infrared Spectra. Polarized infrared surface spectroscopy is a very powerful tool, as it is sensitive to both the chemical nature and the orientation of adsorbates. If the vibrational resonances are well resolved, exquisitely detailed information about the structure of etched surfaces can be obtained by simple analysis of *s*- and *p*-polarized spectra.¹⁵ In contrast, textured or etched surfaces are often more difficult to analyze, as the vibrational modes due to step- and facet-bound species often partially overlap with terrace modes. As a result of this overlap, the vibrational spectra of many etched surfaces are little more than structured “blobs” that defy definitive assignment. In the following, we develop a simple mathematical procedure that can sometimes profoundly simplify complex spectra by taking advantage of the inherent symmetries of the system.

Spectra obtained with *s*-polarized radiation ($\vec{E} \parallel \hat{y}$) are only sensitive to in-plane vibrational components; however, *p*-polarized spectra are more complicated, as the surface electric

field has both in-plane ($\vec{E} \parallel \hat{x}$) and perpendicular ($\vec{E} \parallel \hat{z}$) components. The relative magnitudes of the components of the surface electric field can be calculated from the experimental geometry and the substrate dielectric constant.¹⁶ For the spectra reported here—silicon substrates measured with *s*- and *p*-polarized radiation at 45° incidence in the MIR geometry—the magnitudes of the surface electric field in each direction (i.e. E_x , E_y , and E_z) are comparable; they can be calculated with eqs. 2.6–2.8 in ref 16. In this case, *p*-polarized spectra are *equally sensitive* to in-plane and vertical modes.

To understand the impact of this, consider the hypothetical case of a bulk-terminated Si(100) surface that is entirely covered with vertical SiH₂ groups. By symmetry, this surface should have a *z*-polarized, symmetric Si–H stretch mode and an in-plane-polarized, antisymmetric Si–H stretch mode. Importantly, if these modes overlap in energy, *the z-polarized mode cannot be isolated by traditional polarization analysis*. In this specific case, the *p*-polarized spectrum would display two modes of roughly equal intensity, whereas the *s*-polarized spectrum would display a single mode of comparable intensity. [This statement is not a simple consequence of the surface electric field; the geometry of the Si–H bonds must be included in the calculation.] In the following, we develop a technique that effectively isolates the *z*-polarized component of a spectrum by subtracting all in-plane components from the *p*-polarized spectrum.

In optically thin samples, the intensity of adsorbed infrared radiation is given by

$$I = a(\vec{E} \cdot \vec{\mu})^2 \quad (2)$$

where $\vec{\mu}$ is transition dipole moment of the vibrational mode (summed over all oscillators), \vec{E} is the electric field measured at the surface, and a is a constant. For *s*- and *p*-polarized light, respectively, this becomes

$$I_s = a(E_y \mu_y)^2$$

and

$$I_p = a(E_x \mu_x + E_z \mu_z)^2 \quad (3)$$

In some cases, the inherent symmetry of the surface can be used to simplify eq 3. For example, the Si(100) surface has macroscopic 4-fold rotational symmetry. (Each terrace has only 2-fold symmetry, but the symmetry axis rotates by 90° from one terrace to the next.) As a result, a spectrum obtained with $\vec{E} \parallel \hat{x}$ must be identical to one obtained with $\vec{E} \parallel \hat{y}$. In other words, $\mu_x = \mu_y$. The same is true for Si(111) surfaces, which have 3-fold rotational symmetry, but not for Si(110) surfaces, which have 2-fold rotational symmetry.

In the case where $\mu_x = \mu_y$ by symmetry, *y*- and *z*-polarized spectra (I_y and I_z , respectively) can be calculated from

$$I_y \equiv a\mu_y^2 = \frac{1}{E_y^2} I_s \quad (4)$$

and

$$I_z \equiv a\mu_z^2 = \frac{1}{E_z^2} \left(I_p - \frac{E_x^2}{E_y^2} I_s \right) \quad (5)$$

(Note that the cross-term in eq 3 contains $\mu_x \mu_z$, which is zero

(9) Niwano, M.; Kageyama, J.; Kinashi, K.; Miyamoto, N.; Honma, K. *J. Vac. Sci. Technol. A* **1994**, *12*, 465.

(10) Faggin, M. F.; Hines, M. A. *Rev. Sci. Instrum.* **2004**, *75*, 4547.

(11) Arima, K.; Endo, K.; Kataoka, T.; Oshikane, Y.; Inoue, H.; Mori, Y. *Surf. Sci.* **2000**, *446*, 128.

(12) Kanaya, H.; Usuda, K.; Yamada, K. *Appl. Phys. Lett.* **1995**, *67*, 682.

(13) Endo, K.; Arima, K.; Hirose, K.; Kataoka, T.; Mori, Y. *J. Appl. Phys.* **2002**, *91*, 4065.

(14) Watanabe, S. *Surf. Sci.* **1996**, *351*, 149.

(15) Jakob, P.; Chabal, Y. J. *J. Chem. Phys.* **1991**, *95*, 2897.

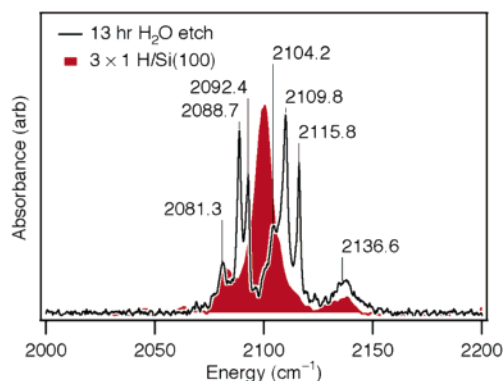


Figure 2. A comparison of the z -polarized spectrum of a Si(100) surface etched for 13 h in deoxygenated H_2O (black line) with that of the $(3 \times 1)\text{-H/Si(100)}$ from ref 18 (red fill). Only the Si–H stretch region is shown.

by symmetry.) Equations 4 and 5 effectively isolate the Cartesian components of the transition dipole moments. In the following, the reported y - and z -polarized spectra are extracted from the raw s - and p -polarized spectra using eqs 4 and 5 and the electric field components calculated from eqs 2.6–2.8 in ref 16.

3.2. Time-Dependent Infrared Spectroscopy. Infrared spectroscopy provides dramatic evidence that simple H_2O etching leads to Si(100) surfaces of remarkable heterogeneity. For example, Figure 2 compares the z -polarized infrared spectrum of a H_2O -etched Si(100) surface to that of the ultrahigh-vacuum-prepared, 3×1 -reconstructed, H-terminated Si(100) surface from ref 17. (The latter spectrum was obtained using the buried metal layer technique which is only sensitive to z -polarized modes.) The $3 \times 1\text{-H/Si(100)}$ surface has been studied extensively with infrared spectroscopy,¹⁸ LEED,¹⁸ and STM¹⁹ and is known to consist of alternating monohydride-terminated dimers (H-Si-Si-H) and dihydride-terminated monomers (SiH_2). In comparison, the H_2O -etched spectrum is notable for two reasons. First, this spectrum is characterized by much narrower line widths—the dominant mode of the UHV-prepared surface is almost 5 times wider than the well resolved modes on the H_2O -etched surface! This implies that the H_2O -etched surface is significantly more homogeneous than the UHV-prepared surface on the few-nm length scale relevant to infrared absorption. Second, the very different spectral signatures of the two H-terminated surfaces imply significantly different surface structures. What surface structure leads to the 7 Si–H stretch bands on the H_2O -etched Si(100) surface?

Infrared spectroscopy also shows that etching is a dynamic process, in agreement with previous studies of $\text{H}_2\text{O/Si(100)}$ etching.²⁰ At room temperature, the etched surface morphology evolves over a period of *days* as shown by Figure 3. At early times, the vibrational features are broad and difficult to resolve. With increased etching, the features sharpen, and new modes emerge. This trend is consistent with the transformation of an initially rough surface to a much more homogeneous surface with well-defined features. Interestingly, the z -polarized spectrum is much sharper and more well resolved than the y -polarized spectrum. For comparison purposes, the positions of the 7 resolved bands observed in the 13-h, z -polarized spectrum

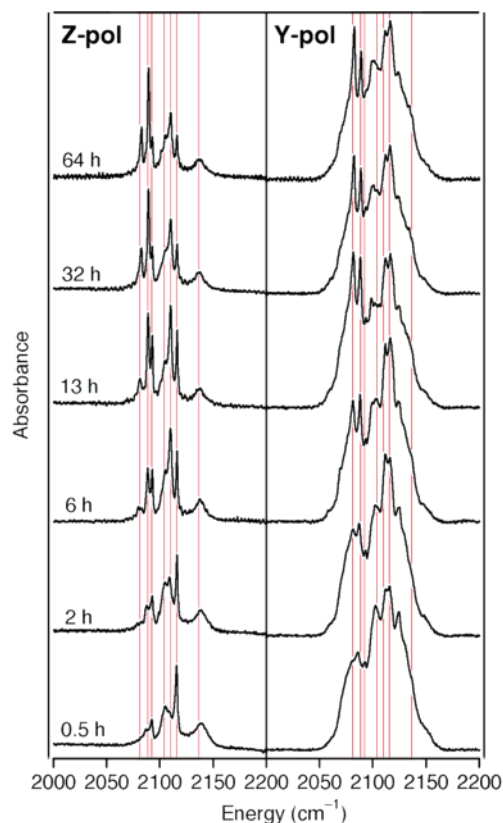


Figure 3. Time-dependent spectra of Si(100) surfaces etched in deoxygenated H_2O . The left and right panels show the z - and y -polarized spectra, respectively. The red lines denote the positions of the 7 labeled features in Figure 2.

are indicated by vertical lines. In the following, we concentrate on the assignment of these features.

The two low-frequency modes at 2081.3 and 2088.7 cm^{-1} are readily assigned to monohydride species adsorbed on Si- $\{111\}$ and Si- $\{110\}$ microfacets as follows. A similarly prepared H_2O -etched Si(111) surface (not shown) displays a single sharp, p -polarized mode at 2083.7 cm^{-1} , which we attribute to a terrace monohydride stretch, in agreement with previous studies of $\text{H}_2\text{O/Si(111)}$ etching.²¹ The 2 cm^{-1} red shift on the (100) surface is attributed to reduced dynamic dipole coupling^{22,23} on microfacets. In comparison, the H/Si(111) stretch vibration on NH_4F -etched surfaces red-shifts by 1.0 cm^{-1} in going from infinite planes to 20 Å-wide, semi-infinite terraces [i.e., flat Si(111) to 9°-miscut Si(111)].²⁴ Similarly, a H_2O -etched Si(110) surface (not shown) displays a sharp p -polarized mode at 2088.7 cm^{-1} and a mixed s - and p -character mode at 2070.3 cm^{-1} , in reasonable agreement with previous studies of $\text{H}_2\text{O/Si(110)}$ etching.¹⁴ These are attributed to the symmetric and antisymmetric stretches of tilted monohydride species bound to ideal Si(110) chains in agreement with studies on NH_4F -etched Si-(110) surfaces.²⁴ Since $\{111\}$ and $\{110\}$ microfacets are tilted by 54.7 and 45° from the (100) surface normal, the 2081.3 and 2088.7 cm^{-1} modes should have significant y - and z -character,

(16) Chabal, Y. J. *Surf. Sci. Rep.* **1988**, *8*, 211.

(17) Noda, H.; Urisu, T. *Chem. Phys. Lett.* **2000**, *326*, 163.

(18) Chabal, Y. J.; Raghavachari, K. *Phys. Rev. Lett.* **1985**, *54*, 1055.

(19) Boland, J. J. *Surf. Sci.* **1992**, *261*, 17.

(20) Kanaya, H.; Usuda, K.; Yamada, K. *Appl. Phys. Lett.* **1995**, *67*, 682.

(21) Watanabe, S.; Nakayama, N.; Ito, T. *Appl. Phys. Lett.* **1991**, *59*, 1458.

(22) Jakob, P.; Chabal, Y. J.; Raghavachari, K. *Chem. Phys. Lett.* **1991**, *187*, 325.

(23) Newton, T. A.; Boiani, J. A.; Hines, M. A. *Surf. Sci.* **1999**, *430*, 67.

(24) Jakob, P.; Chabal, Y. J.; Kuhnke, K.; Christman, S. B. *Surf. Sci.* **1994**, *302*, 49.

whereas the 2070.3 cm^{-1} mode should be y -polarized. This explains the absence of a 2070.3 cm^{-1} mode in z -polarized spectra.

In the assignment process, we next consider other well characterized H/Si(100) structures—the 1×1 ,¹⁸ 2×1 ,²⁵ and 3×1 ¹⁸ reconstructions, which are typically prepared by exposing clean Si(100) surfaces to an atomic H source in ultrahigh vacuum. All three reconstructions contain H-terminated Si dimers (H–Si–Si–H); the 1×1 and 3×1 reconstructions also contain dihydride-terminated monomers (SiH₂). The 1×1 and 3×1 reconstructions differ primarily in their degree of order;¹⁹ these surfaces have nearly identical infrared spectra.¹⁸ [Note that an unreconstructed, dihydride-terminated H/Si(100) surface, which would also give a 1×1 diffraction pattern, has never been experimentally observed.] Importantly, all three of these surfaces display strong p -polarized absorption bands centered at 2099 – 2100 cm^{-1} . As illustrated by Figure 2, a band of this type is entirely absent in our spectra. We therefore conclude that *there is no silicon dimerization on the H₂O-etched surface.*

A careful examination of the z -polarized spectra in Figure 3 shows that the intensities of some absorption bands are highly correlated, suggesting that the correlated bands arise from the same structural unit (e.g., in-phase and out-of-phase vibrations of a SiH₂ species). Importantly, the intensity variations are not accompanied by significant shifts in line position. From this, we conclude that the spectral intensities are not complicated by “intensity borrowing.”²⁶ Changes in the integrated intensity of any one band should thus reflect changes in population of the structural unit. Of course, the integrated intensities cannot be converted into absolute populations without additional information on the oscillator strength and geometry of the vibrational mode.

To investigate these correlations, the integrated intensity of each band was estimated from a global fit of the time-dependent z -polarized spectra to 7 overlapping Gaussians. The results of this procedure for the 6 well-resolved modes are displayed in Figure 4a–d. The bottom panel of Figure 4 shows the integrated intensity of $I_z + 2I_y$ over the entire Si–H stretch region (2055 – 2155 cm^{-1}). In the absence of chemically induced changes in Si–H oscillator strength (i.e., if all Si–H bonds have the same dynamic dipole moment), this quantity is a direct measure of H coverage *irrespective* of any dynamic dipole coupling. Although etching may change the surface roughness and thus the exposed surface area, the total number of Si–H units on the surface will remain constant as long as the etchant does not undercut the surface or form vertical features. Therefore, the nearly constant value of this integral with time confirms the quantitative validity of this approach.

Figure 4a shows that the integrated intensities of the two highest frequency modes, which are centered at 2115.8 and 2136.6 cm^{-1} , are strongly correlated, as are the intensities of the bands at 2092.4 and 2109.8 cm^{-1} , which are displayed in Figure 4b. In contrast, the bands assigned to Si{111} and Si{110} microfacets have distinctly different intensity patterns, as seen in Figure 4c,d. Unfortunately, spectral congestion in the y -polarized spectra prohibits a similar analysis of the in-plane intensities, which would have allowed for a definitive

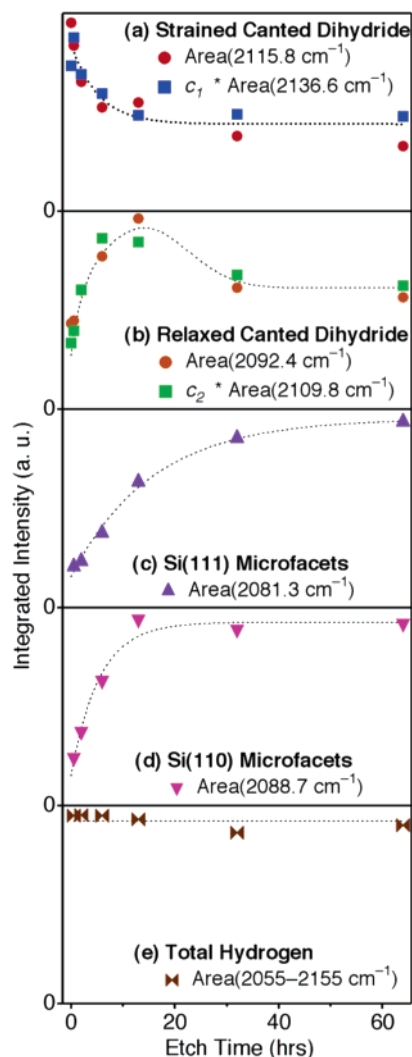


Figure 4. (a–d) Time-dependent integrated intensities of the 6 well-resolved spectral lines in the z -polarized spectra in Figure 3; the lines are meant as a guide. (e) Integrated intensity of the entire Si–H stretch region; the line represents the average integral. The relative intensities of any two features cannot be meaningfully compared without additional geometrical knowledge. To illustrate correlations in intensity, the low frequency features in (a) and (b) were scaled by arbitrary constants, c_1 and c_2 .

determination of the dynamic dipole orientations. Nevertheless, all four of the correlated bands appear to have significant in-plane and out-of-plane character.

These features cannot be explained by an unreconstructed, bulk-terminated surface, in which every surface atom is terminated by a symmetric dihydride (SiH₂), for two reasons. First, this geometry is chemically unrealistic, as the spacing between H's on adjacent dihydrides²⁷ would be only 1.51 \AA —far below a H atom's 2.4 \AA van der Waals diameter. Indeed, calculations have shown that the symmetric dihydride structure is not thermodynamically preferred.²⁷ Second, this termination would give rise to a z -polarized symmetric stretch and an in-plane-polarized antisymmetric stretch, which is inconsistent with the mixed-polarization character of the four unassigned modes. This argument also rules out the possibility of a high density of isolated dihydrides (e.g., isolated atoms on flat terraces) or

(25) Chabal, Y. J.; Raghavachari, K. *Phys. Rev. Lett.* **1984**, *53*, 282.

(26) Hollins, P.; Pritchard, J. *Prog. Surf. Sci.* **1985**, *19*, 275.

(27) Northrup, J. E. *Phys. Rev. B: Condens. Matter Mater. Phys.* **1991**, *44*, 1419.

one-atom-wide stripes of dihydrides, such as those suggested by Endo, et al.¹³

As first pointed out by Ciraci and Batra²⁸ and later confirmed by other calculations,^{27,29–31} the steric problems with the bulk-terminated H/Si(100) surface can be relieved by tilting each SiH₂ and slightly increasing its bond angle to form a *strained canted dihydride* structure. Although there is significant disagreement among the calculations as to the magnitude of the distortion (e.g., the tilt angle), the vibrational mode frequencies and their polarizations,³² the calculations all predict the appearance of two uncoupled vibrational modes due to localized stretches of the two inequivalent Si–H bonds.

There is also experimental precedent for a canted dihydride structure. When Si(111) surfaces miscut toward the $\langle\bar{1}\bar{1}2\rangle$ direction are etched in NH₄F, a H-terminated surface with relatively straight, dihydride-terminated steps is produced.¹⁵ Steric interactions between the step dihydride and a monohydride bound to the terrace below the step lead to the canting of the dihydride moiety.³³ As a result, three Si–H stretch modes are observed—two from the independent motion of the dihydride bonds and one from the motion of the strained terrace monohydride.³⁴ The sterically hindered dihydride mode, known as C₃, occurs at 2134.7 cm⁻¹, whereas the unhindered dihydride mode, C₁, occurs at 2093.6 cm⁻¹.¹⁵

In principle, isolated trihydride species, which would be tilted by ~55° on a (100) surface, could also give rise to a pair of mixed-polarization vibrational modes. Indeed, SiH₃ vibrational modes in the 2120–2140 cm⁻¹ range have been predicted by ab initio calculations.³⁵ We discount this possibility for three reasons. First, similar modes are entirely absent from H₂O-etched Si(110) and Si(111) surfaces (not shown). It is unlikely that H₂O would rapidly etch isolated atoms on the (110) and (111) surfaces while leaving a high concentration of these species on the (100) surface. Second, the narrow line width of the 2115.8 cm⁻¹ mode suggests that this species is in a highly homogeneous environment, whereas a random distribution of isolated atoms would likely display significant heterogeneous broadening. Third, we find no evidence of isolated atoms in STM images (vide infra), which is inconsistent with the relatively strong intensity of these modes.

On the basis of the above considerations, we assign the remaining four well-resolved modes to two types of asymmetric (canted) dihydrides:³⁶ a strained canted dihydride that absorbs at 2115.8 and 2136.6 cm⁻¹ and a somewhat relaxed canted dihydride species that absorbs at 2092.4 and 2109.8 cm⁻¹. This assignment is consistent with the generally observed trend that higher strain gives rise to higher frequency Si–H stretch vibrations and larger SiH₂ mode splittings.

Table 1. Energies and Mode Assignments of Si–H Stretch Modes Observed on Si(100) Surfaces Etched in Deoxygenated H₂O for 13 h

energy (cm ⁻¹)	assignment
2081.3	monohydride on (111) microfacet
2088.7	monohydride on (110) microfacet
2092.4	relaxed canted (100) dihydride (ν_{ss})
2109.8	relaxed canted (100) dihydride (ν_{as})
2115.8	strained canted (100) dihydride (ν_{ss})
2136.6	strained canted (100) dihydride (ν_{as})

The observed absorption frequencies and their mode assignments are collected in Table 1.

With these mode assignments in hand, infrared spectroscopy provides a very detailed picture of the chemical state and temporal evolution of the water-etched surface. The starting surface is very heterogeneous and characterized by a preponderance of sterically hindered dihydride species, as would be expected of a bulk-terminated Si(100) surface. Water etching profoundly changes the chemical state of the surface, selectively removing strained dihydride features and introducing less-strained dihydrides. At the same time, etching produces {111} and {110} microfacets that grow with increasing etch time. In spite of this level of detail, infrared spectroscopy leaves a number of questions unanswered. For example, do the {111} and {110} microfacets decorate etch hillocks, etch pits, or both? What is the characteristic size of these facets? Does increased etching increase the size of the facets or simply produce more facets? And most importantly, is this spectral homogeneity (e.g., narrow line widths) associated with atomically flat regions of the surface? To answer these questions, a technique sensitive to long-range structure, such as STM, is required.

3.3. Scanning Tunneling Microscopy. The morphologies of water-etched Si(100) surfaces were studied with STM. [We note that other researchers have used STM to study H₂O-etched surfaces displaying much broader H/Si(100) vibrational spectra.^{11–13}] As expected, the highly aggressive cleaning solutions used in sample preparation produced very rough initial surface morphologies (not shown) with no discernible atomic-scale features, such as step edges or etch pits. In agreement with the spectroscopic data, extended water etching produced surprisingly smooth and homogeneous etched surfaces. For example, the smoothest surfaces were produced after ~11 h of etching as illustrated by the STM images in Figure 1. These surfaces display three characteristic morphological features:

- Nearly straight step edges running in two orthogonal directions—the [010] and [001] directions (i.e., +45 and -45° in Figure 1),
- Stripes of *atomically flat Si(100)* bounded by straight step edges and terminated by etch hillocks, and
- Multilayer hillocks with a roughly square footprint and flattened top. Although tip effects complicate geometrical analyses, these images are consistent with the production of roughly pyramidal hillocks.

This morphology is qualitatively consistent with the spectroscopic analysis presented in the previous section. First, the stripes of atomically flat Si(100) as well as the relatively large regions of flat terrace are consistent with the production of sharp, well-resolved, silicon dihydride stretch modes. Second, the orientation and square habit of the multilayer hillocks, which is reflected in the 4-fold symmetry of the stripes, is consistent

(28) Ciraci, S.; Batra, I. P. *Surf. Sci.* **1986**, *178*, 80.

(29) Tagami, K.; Tsukuda, M. *Surf. Sci.* **1997**, *384*, 308.

(30) Tagami, K.; Tsuchida, E.; Tsukuda, M. *Surf. Sci.* **2000**, *446*, L108.

(31) Freking, U.; Krüger, P.; Mazur, A.; Pollmann, J. *Phys. Rev. B: Condens. Matter Mater. Phys.* **2004**, *69*, 035315.

(32) The apparent origins of this disagreement are discussed in ref 31.

(33) Raghavachari, K.; Jakob, P.; Chabal, Y. J. *Chem. Phys. Lett.* **1993**, *206*, 156.

(34) Hines, M. A.; Chabal, Y. J.; Harris, T. D.; Harris, A. L. *Phys. Rev. Lett.* **1993**, *71*, 2280.

(35) Burrows, V. A.; Chabal, Y. J.; Higashi, G. S.; Raghavachari, K.; Christman, S. B. *Appl. Phys. Lett.* **1988**, *53*, 998.

(36) The formation of two distinct dihydride species on Si(100) was suggested in an earlier study of pH-dependent Si(100) etching (Dumas, P.; Chabal, Y. J.; Jakob, P. *Surf. Sci.* **1992**, *269/70*, 867); however, the mode frequencies observed in that study are significantly different from those observed here.

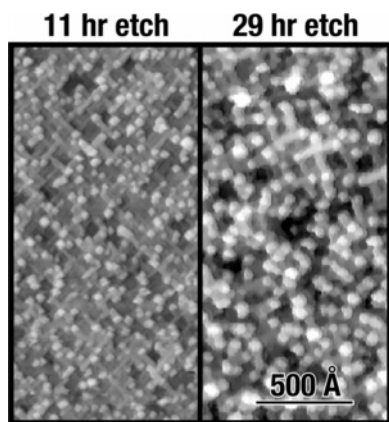


Figure 5. STM images of two surfaces etched for 11 (left) and 29 h (right) in deoxygenated H_2O . The lateral and vertical scales are identical. Extended etching increases the size and density of the hillocks at the expense of the stripes.

with the production of hillocks bounded by $\text{Si}\{111\}$ microfacets. Smaller $\{111\}$ microfacets also bound the flat $\text{Si}(100)$ stripes. Third, the hillocks are not truly square pyramidal; instead, their vertexes are somewhat rounded. This rounding is consistent with the formation of $\text{Si}\{110\}$ microfacets with Si chains running parallel to the vertexes. The $\{110\}$ microfacets appear somewhat rounded, suggesting some contribution from vicinal $\{110\}$ surfaces.

To understand the temporal evolution of the site densities observed in the spectroscopic measurements, the time-dependent etch morphology was studied. Figure 5 directly compares the morphologies of surfaces etched for 11 and 29 h. Two effects are readily apparent. First, the width, height and density of the hillocks all increase with increasing etch time. This result is consistent with the increased intensity of the hillock-associated modes—those from the $\{111\}$ and $\{110\}$ microfacets—and the reduced intensity of the dihydride stretch modes seen for longer etch times. Second, the $\text{Si}(100)$ stripes seen after the 11 h etch are much reduced, although still visible, after a 29 h etch. This observation is also consistent with the reduced intensity of the dihydride stretch modes after extended etching.

One question remains unanswered—how do the strained and relaxed dihydride species differ from one another and where are the two distinct dihydride species located? The relatively narrow line widths of the dihydride-related features suggests that both species occur in relatively homogeneous patches. The significant shifts in frequency and in splitting suggest that the difference between these species is not subtle; one species appears to be much less strained than the other. Furthermore, although the relative spectral areas of these features cannot be quantitatively compared, their comparable absorption intensities suggest that both species have a significant surface concentration. A comparison of the surface densities derived from the infrared spectra and the morphological data suggests that the relaxed dihydride species, which reaches a maximum surface density after ~ 12 h of etching, is associated with the flat $\text{Si}(100)$ stripes. The stripes are completely absent from the starting surface and most apparent on the surface etched for 12 h. Longer etch times produce surfaces with a higher hillock density and fewer stripes. The strained dihydride species is therefore assigned to canted dihydrides on the flat etched terraces.

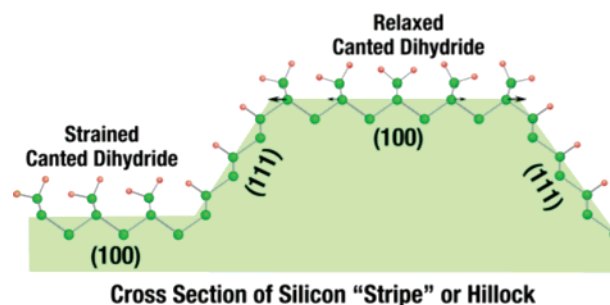


Figure 6. Schematic diagram of the proposed atomic scale structure of the etched surface, showing the cross section of a flat terrace (left) and a stripe or hillock (right). The arrows indicate possible relaxation of the lattice to relieve strain.

4. Discussion

These results raise two questions. First, why are the dihydrides bound to the silicon stripes relaxed, whereas those on the flat $\text{Si}(100)$ surface remain highly strained? Second, why do the stripes have a characteristic width (~ 25 Å in Figure 1)? We suggest that these two questions are correlated and that stripe formation is driven by *stress relief*. On a flat $\text{Si}(100)$ surface, the canted dihydride reconstruction relieves some of the stress between adjacent dihydrides, but not all. Complete stress relief would require a uniaxial expansion of the entire silicon lattice, which is energetically unfeasible. The situation is different on the top of a nanoscale stripe. If the dihydride units are oriented such that the Si–H bonds are perpendicular to the long axis of the stripe, the steric stress could be relieved in two ways, as sketched in Figure 6. The first is by the generation of a two-domain structure on the stripe, with dihydrides tilting toward the nearest edge, similar to structures found in previous molecular dynamics simulations.³⁷ The second is by a small expansion of the lattice in the direction parallel to the short axis of the stripe, as suggested by the arrows in Figure 6. (The figure is somewhat misleading, as this type of relaxation extends down a number of atomic layers.) Both types of relaxation would also be allowed on hillock apexes, suggesting two locations for the relaxed dihydride species.

Uniaxial relaxation of nanoscale stripes and hillocks (or “dots”) is well-known in heteroepitaxy, where strain is induced by the lattice mismatch between the substrate and overlayer. For example, when Ag is deposited on $\text{Si}(100)$, the silver atoms spontaneously self-assemble into microns-long, one-dimensional “quantum wires.”³⁸ This shape allows elastic relaxation of the island’s stress in the direction parallel to the short axis of the wires. A similar phenomenon is seen in the growth of Ge on $\text{Si}(100)$ ³⁹ where the same general mechanism leads to the formation of rectangular “hut clusters.”⁴⁰ In the case of H_2O etched surfaces, the stress would be induced by steric interactions between adjacent dihydrides.

There is a significant difference between stress-driven island formation in heteroepitaxy and stripe formation during the etching of $\text{Si}(100)$. In the former, the heteroatoms are free to diffuse across the surface, whereas there is no surface diffusion of silicon during room-temperature etching. In the case of silicon etching, the production of nanoscale stripes (and hillocks) must

(37) Tagami, K.; Tsukada, M. *Surf. Sci.* **1998**, *400*, 383.

(38) Tersoff, J.; Tromp, R. M. *Phys. Rev. Lett.* **1993**, *70*, 2782.

(39) Eaglesham, D. J.; Cerullo, M. *Phys. Rev. Lett.* **1990**, *64*, 1943.

(40) Mo, Y.-W.; Savage, D. E.; Swartzentruber, B. S.; Lagally, M. G. *Phys. Rev. Lett.* **1990**, *65*, 1020.

be driven by the different reactivities of the various surface species. For example, the temporal evolution of the surface dihydrides seen in Figure 4, whereby unstrained dihydrides increase in intensity at the expense of strained dihydrides, strongly suggests that the *strained dihydrides are more reactive than the relaxed dihydrides*.

The novel aspect of this system is that an atomically flat (100) surface terminated entirely by relaxed dihydrides cannot be formed, as stress relaxation requires nanometer-width domains. The etch morphology is likely influenced by the rough nature of the starting surface as well. Since the initial surface has no preferred direction, the etchant can initially form nanometer-width rectangles of both orientations. These domains cannot grow indefinitely along their long axis, though, as they invariably intersect a domain with the opposite orientation. In the end, these intersecting rectangles and frustrated etching lead to a surface morphology reminiscent of Mondrian.⁴¹ Although homogeneous on the atomic-scale, the surface assumes a hill-and-valley, faceted morphology in a kinetic attempt to minimize surface stress. With this in mind, it would be interesting to study the etching of surfaces with broken symmetry (e.g., miscut surfaces, uniaxially textured surfaces.)

This type of kinetic, stress-induced roughening has an equilibrium analogue that has been well studied on clean Si(100) surfaces. On a clean surface, two adjacent atoms can lower their energy by dimerizing; however, this dimerization produces a compressive stress. (This stress is in some sense the reverse of the tensile stress produced by neighboring SiH₂ groups on the H-terminated surface.) Because of this, an atomically flat dimerized surface (where all of the dimers are parallel) would be subject to an immense, macroscopic uniaxial strain. To minimize this effect, the energetically preferred structure consists of alternating stress domains with dimers running parallel and perpendicular to the [010] direction.⁴² Macroscopically, this arrangement minimizes the effects of strain. The existence of stress domains has been confirmed by very elegant experiments on the structure of stressed Si(100) surfaces.⁴³ Would macroscopic stress have a similar effect on the morphology of etched Si(100) surfaces?

The production of atomically straight steps, such as those bounding the stripes, also has implications about the reactivity of the etchant. As we have shown in previous experimental and computational studies of Si(111) etching,⁴ atomically straight steps are produced by highly anisotropic etchants that etch kink sites much more rapidly than step sites. Interestingly, this observation suggests that H₂O will be a step flow etchant of vicinal Si(100) surfaces.

Unfortunately, the steady-state H₂O-etched surface morphology cannot be predicted from these simple arguments, and many questions remain unanswered. For example, the shape of the etch hillocks is very interesting. Simple geometric arguments⁴⁴

suggest that etch hillocks should always be bounded by slow etching faces, such as (111) microfacets. In this case, infrared spectroscopy clearly shows a significant contribution from (110) surfaces as well, even though Si(110) is typically the fastest etching surface. The origin of this discrepancy is simple—the simple geometric prediction ignores the etching of edges and vertexes. Geometric arguments may work on micron-scale hillocks, but edge and vertex sites make up a significant fraction of a nanoscale hillock. Similarly, the dramatic increase in hillock density with increasing etch time is not understood. Why do hillocks nucleate in the first place? Some have argued that hillock nucleation is due to heterogeneity in the system (e.g., H₂ bubbles produced by the etching reaction,⁴⁵ precipitated siliceous etch products.⁴⁶) Although we cannot rule this out, Figure 5 shows that although the hillocks increase in size with etch time, the size distribution remains relatively narrow. This suggests an intrinsic mechanism. To answer these questions, a computer simulation of H₂O/Si(100) etching is under development.

5. Conclusions

The etching of Si(100) surfaces in deoxygenated H₂O leads to time-dependent surface morphologies. After extended etching (~12 h) at room temperature, this process produces H-terminated Si(100) surfaces of remarkable atomic-scale homogeneity, as evidenced by infrared spectroscopy, but significant nanoscale heterogeneity, as evidenced by scanning tunneling microscopy. In contrast to vacuum-prepared H-terminated Si(100) surfaces, there is no evidence of dimerization on the H₂O-etched surfaces. Instead, atomically flat regions of the surface are terminated by a strained canted dihydride structure, in agreement with previous theoretical predictions. The unusual hill-and-valley structure of the etched surface is attributed to the effects of strain on the reactivity of individual sites on the etched surface. In particular, large atomically flat regions are unstable to further etching, as steric interactions between neighboring canted dihydrides lead to increased reactivity. Because of this, the etched surface is characterized by nanoscale “stripes” terminated by a relatively unstrained (or relaxed) dihydride and hillocks bounded by {111} and {110} microfacets and capped with relaxed dihydrides.

Acknowledgment. M.F.F., I.T.C., and M.A.H. gratefully acknowledge support by the NSF under Award No. CHE-0515436 and by the Center for Nanoscale Systems (NSF EEC-0117770). K.T.Q. and S.K.G. gratefully acknowledge support from a Research Corporation College Science Award and a Camille and Henry Dreyfus Faculty Start-up Award.

JA062172N

(41) <<http://www.artmuseums.harvard.edu/mondrian/>>

(42) Alerhand, O. L.; Vanderbilt, D.; Meade, R. D.; Joannopoulos, J. D. *Phys. Rev. Lett.* **1988**, *61*, 1973–6.

(43) Webb, M. B.; Men, F. K.; Swartzentruber, B. S.; Kariotis, R.; Lagally, M. G. *Surf. Sci.* **1991**, *242*, 23–31.

(44) Batterman, B. W. *J. Appl. Phys.* **1957**, *28*, 1236.

(45) Palik, E. D.; Glembocki, O. J.; Heard, Jr. I.; Burno, P. S.; Tenez, L. *J. Appl. Phys.* **1991**, *70*, 3291.

(46) Nijdam, A. J.; van Veenendaal, E.; Cuppen, H. M.; van Suchtelen, J.; Reed, M. L.; Gardeniers, J. G. E.; van Enkevort, W. J. P.; Vlieg, E.; Elwenspoek, M. *J. Appl. Phys.* **2001**, *89*, 4113.